TENSION ESTIMATION METHODS FOR NIELSEN-LOHSE BRIDGES USING OUT-OF-PLANE AND IN-PLANE NATURAL FREQUENCIES

*Aiko Furukawa[1], Satoshi Yamada[1] and Ryosuke Kobayashi[2]

[1]Department of Urban Management, Kyoto University, Japan; [2]Kobelco Wire Company, Ltd., Japan

*Corresponding Author, Received: 20 Jan. 2022, Revised: 26 May 2022, Accepted: 06 June 2022

ABSTRACT: Nielsen-Lohse bridges are tied-arch bridges, in which braced cables cross each other and are connected by intersection clamps. In the maintenance of Nielsen-Lohse bridges, cable tension has to be estimated for safety evaluation. In the current practice for cable tension estimation, the intersection clamps are removed, a vibration-based cable tension estimation method for single cables is applied to each cable, and the intersection clamps are then reinstalled. However, the removal and reinstallation of the intersection clamps take time and labor. To improve the efficiency of the tension estimation procedure, the authors proposed two tension estimation methods (methods 1 and 2) for two cables connected by the intersection clamp in a previous study. Method 1 uses the natural frequencies in the out-of-plane direction, while method 2 uses the natural frequencies in the in-plane direction. Methods 1 and 2 require at least four and six natural frequencies in the out-of-plane and in-plane directions, respectively. However, collection of the required number of natural frequencies in each direction and specification of the vibration direction for each natural frequency can occasionally be difficult. With this background, the first objective of this study is to propose two additional methods (methods 3 and 4) that allow simultaneous input of both the out-of-plane and in-plane natural frequencies. The difference between the methods is that method 3 requires the vibration direction for each natural frequency but method 4 does not. The second objective of this study is to compare the validity of the four methods (methods 1, 2, 3, and 4), and to examine which method is recommended in which situation through numerical and experimental verifications. It was concluded that method 1 is recommended if the vibration direction of measured out-of-plane natural frequencies is assigned correctly, and method 4 is recommended if the vibration direction of the measured natural frequencies is assigned wrongly. Out-of-plane natural frequencies were found to be more reliable because out-of-plane vibrationallows are easier to generate.

Keywords: New cable tension estimation method, Nielsen-Lohse bridge, Natural frequency, Out-of-plane direction, In-plane direction, Vibration direction

1. INTRODUCTION

Cable structures such as those in cable-stayed bridges are designed to support loads using cable tension. Because each cable has a specific load-bearing capacity, it is necessary to measure cable tension and confirm that the cable does not exceed its load-bearing capacity. The cable tension can be measured by a direct measurement method using devices such as load cells or by an indirect estimation method using the cable's vibration characteristics. The former method is difficult to apply in practical situations because of the high cost and installation of complex devices. Therefore, the latter method is generally used in practice because it is simpler to implement.

In Japan, the vibration method proposed by Shinke et al. [1] and the higher-order vibration method proposed by Yamagiwa et al. [2] are mainly used in practice of cable tension estimation. Shinke et al. [1] modeled the cable under test as a string and proposed an equation to estimate its tension from the natural frequency of a single mode. However, because an actual cable is not a perfect string and its bending stiffness thus cannot be ignored, a correction formula was proposed that takes the effect of the bending stiffness into account. Therefore, it is necessary to determine the cable's bending stiffness value in advance. This problem was solved in the higher-order vibration method of Yamagiwa et al. [2]. In this method, the cable was modeled as a tensioned Euler-Bernoulli beam, and a theoretical equation to express the natural frequency of each mode was derived using the tension and bending stiffness. Therefore, if the natural frequencies of two or more modes are measured, it becomes possible to estimate the tension and the bending stiffness simultaneously. It is thus no longer necessary to determine the bending stiffness in advance.

In addition to the methods above, several other tension estimation methods have been proposed, including a method that uses mode shapes [3], a method for cables with complex boundary

conditions [4] [5], a method for inclined cables [6], a method that uses a neural network [7], and methods for cables with a damper [8] [9] [10]. However, these studies address tension estimation for a single cable.

This study focuses on estimation of the tension of two cables connected using an intersection clamp on a Nielsen-Lohse bridge [11] [12] [13], which is illustrated in Fig. 1. The girder is supported elastically by bracing cables suspended from the arch members. These braced cables cross each other and are connected using intersection clamps to prevent noise and damage being caused by contact due to wind-induced vibration.

In the current cable tension estimation practice for Nielsen-Lohse bridges, single cable tension estimation methods such as the vibration method [1] or the higher-order vibration method [2] are used after the intersection clamps are removed to allow each cable to vibrate as a single cable. However, because the intersection clamps are often installed high above the girders, their removal and re-installation requires use of an aerial working platform and traffic control, which requires additional time and labor. Therefore, if the tension can be estimated without removal of the intersection clamps, the tension estimation process efficiency will be improved.

There have been few previous studies on tension estimation methods for Nielsen-Lohse bridges. Kuriyama et al. [14] proposed a method in which the length of cable between the intersection clamp and one cable end is regarded as a single cable, and the higher-order vibration method is applied without removing the intersection clamp. However, because these intersection clamps are not fixed, it is difficult to regard an intersection clamp theoretically as an end. Therefore, a method based on an overall model of the connected cables and the intersection clamp is required. However, such a method has yet to be studied.

The authors recently proposed two methods (methods 1 and 2) to estimate the tension of two cables connected using an intersection clamp from the natural frequencies [15]. Method 1 uses the natural frequencies in the out-of-plane direction, and the tensions and bending stiffnesses of the two cables are estimated simultaneously. Therefore, at least four natural frequencies are required in the out-of-plane direction. Method 2 uses the natural frequencies in the in-plane direction, and the tensions, bending stiffnesses, and axial stiffnesses of two cables are estimated simultaneously. Therefore, at least six natural frequencies are required in the in-plane direction.

However, collection of the required number of natural frequencies in each direction can occasionally be difficult. Additionally, there are cases in which specification of the vibration direction for each natural frequency is difficult. Therefore, this study proposes two additional methods, designated methods 3 and 4, which allow simultaneous input of the out-of-plane and in-plane natural frequencies. The difference between these methods is that method 3 requires the vibration direction for each natural frequency but method 4 does not require these directions. The validity of both of the proposed methods was verified via numerical simulations and laboratory experiments.

2. TENSION ESTIMATION METHODS

This section explains the authors' previously proposed tension estimation methods (designated methods 1 and 2) and the newly proposed methods (designated methods 3 and 4).

2.1 Definition of Axis and Displacements

This study deals with methods to estimate the tensions of two cables connected using an intersection clamp, as illustrated in Fig. 2(a). It is assumed that both ends of the cables are simply supported. Assuming that there is a plane that consists of the two cables, the vibrations of the cables can be divided into two directions: vibrations perpendicular to the plane (the out-of-plane direction) and vibrations in the plane (the in-plane direction).

A cable number k ($k = 1,2$) is assigned to each of the two cables. The elemental coordinate system used for cable k is shown in Fig. 2(b).
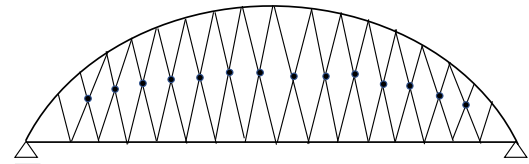
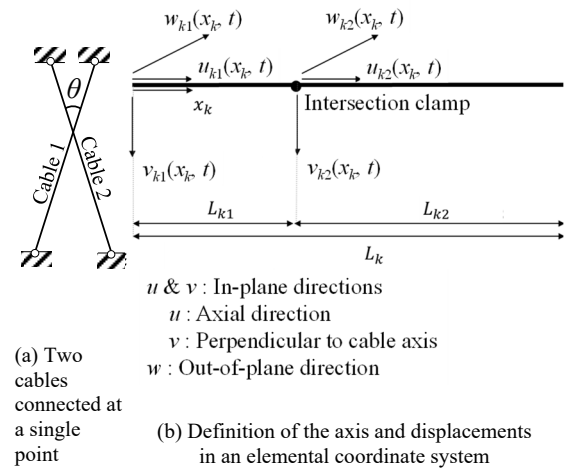Fig. 1 Schematic view of Nielsen-Lohse bridge

(a) Two cables connected at a single point

(b) Definition of the axis and displacements in an elemental coordinate system

u & v : In-plane directions
u : Axial direction
v : Perpendicular to cable axis
w : Out-of-plane direction

Fig. 2 Target model

The cable axis is x_k, and the right direction represents the positive direction. Let m be the index that represents the left side $(m = 1)$ and the right side $(m = 2)$ of the intersection clamp. Let the length from the left end to the intersection clamp be L_{k1}, and let the length from the intersection clamp to the right end be L_{k2}; then, the cable length L_k is $L_k = L_{k1} + L_{k2}$.

2.2 Vibration Equation

By considering the cable to be a tensioned Euler-Bernoulli beam, the vibration equations for the three directions are expressed as the following partial differential equations.

$$\rho_k A_k \frac{\partial^2 w_{km}(x_k,t)}{\partial t^2} + E_k I_k \frac{\partial^4 w_{km}(x_k,t)}{\partial x_k^4} \\ - T_k \frac{\partial^2 w_{km}(x_k,t)}{\partial x_k^2} = 0 \tag{1}$$

$$\rho_k A_k \frac{\partial^2 u_k(x_k,t)}{\partial t^2} - E_k A_k \frac{\partial^2 u_k(x_k,t)}{\partial x_k^2} = 0 \tag{2}$$

$$\rho_k A_k \frac{\partial^2 v_{km}(x_k,t)}{\partial t^2} + E_k I_k \frac{\partial^4 v_{km}(x_k,t)}{\partial x_k^4} \\ - T_k \frac{\partial^2 v_{km}(x_k,t)}{\partial x_k^2} = 0 \tag{3}$$

where $w_{km}(x_k, t)$ is the out-of-plane displacement of cable k on the left $(m = 1)$ or right $(m = 2)$ side with regard to position x_k and time t. $u_{km}(x_k,t)$ and $v_{km}(x_k,t)$ are the in-plane displacements. $u_{km}(x_k,t)$ is the axial displacement and $v_{km}(x_k,t)$ is the displacement orthogonal to the axis. ρ_k is the cable material density, A_k is the cross-sectional area, $\rho_k A_k$ is the mass per unit length, E_k is Young's modulus, I_k is the second moment of area, $E_k I_k$ is the bending stiffness, $E_k A_k$ is the axial stiffness, and T_k is the tension of cable k.

$w_{km}(x_k,t)$, $u_{km}(x_k,t)$, and $v_{km}(x_k,t)$ are given by the product of a function of the cable coordinate x_k and a function of time t, as follows:

$$w_{km}(x_k,t) = W_{km}(x_k)\exp{(j\omega t)} \tag{4}$$

$$u_{km}(x_k,t) = U_{km}(x_k)\exp{(j\omega t)} \tag{5}$$

$$v_{km}(x_k,t) = V_{km}(x_k)\exp{(j\omega t)} \tag{6}$$

2.3 Constraint Equations for Natural Frequencies in the Out-of-Plane Direction [15]

Substitution of Eq. (4) into Eq. (1) allows the ordinary differential equation for $W_{km}(x_k)$ to be obtained. The general solution for $W_{km}(x_k)$ is then obtained by solving this ordinary differential equation. By applying the boundary conditions at both ends of the cable, and applying the continuity

conditions and the equilibrium of forces at the intersection clamp position to the general solution, the following constraint equation for the natural frequency f_i of the ith mode can be derived.

$$G_1^i \equiv g_{11}^i g_{22}^i + g_{12}^i g_{21}^i \frac{g_{32}^i}{g_{31}^i} = 0 \tag{7}$$

The functions that compose the function G_1^i and its related functions are given as follows.

$$g_{1k}^i = \sin \alpha_k^i L_k \tag{8}$$

$$g_{2k}^i = \sin \alpha_k^i L_{k1} \sin \alpha_k^i L_{k2} \\ - \frac{\alpha_k^i}{\beta_k^i} \sin \alpha_k^i L_k \frac{1 + e^{-2\beta_k^i L_k} - e^{-2\beta_k^i L_{k1}} - e^{-2\beta_k^i L_{k2}}}{2(1 - e^{-2\beta_k^i L_k})} \tag{9}$$

$$g_{3k}^i = E_k I_k \left\{ \left(\alpha_k^i\right)^2 + \left(\beta_k^i\right)^2 \right\} \alpha_k^i \tag{10}$$

$$\alpha_k^i = \sqrt{\sqrt{\left(\frac{T_k}{2E_k I_k}\right)^2 + \frac{\rho_k A_k (2\pi f_i)^2}{E_k I_k}} - \frac{T_k}{2E_k I_k}} \tag{11}$$

$$\beta_k^i = \sqrt{\sqrt{\left(\frac{T_k}{2E_k I_k}\right)^2 + \frac{\rho_k A_k (2\pi f_i)^2}{E_k I_k}} + \frac{T_k}{2E_k I_k}} \tag{12}$$

The natural frequency f_i is not included explicitly in Eq. (7), but it is included in α_k^i and β_k^i in Eqs. (11) and (12). In conclusion, Eq. (7) represents the constraint equation that f_i in the out-of-plane direction must satisfy.

2.4 Constraint Equations for Natural Frequencies in the In-Plane Direction [15]

Substitution of Eqs. (5) and (6) into Eqs. (2) and (3) allows the ordinary differential equations for $u_{km}(x_k,t)$ and $v_{km}(x_k,t)$ to be obtained. General solutions for $U_{km}(x_k)$ and $V_{km}(x_k)$ can then be obtained by solving the ordinary differential equations. By applying the boundary conditions at both ends of the cable and the continuity conditions and the equilibrium of forces at the intersection clamp position to the general solutions, the following constraint equation for the natural frequency f_i of the i-th mode can be derived:

$$G_2^i \equiv$$
$$\cos^2\theta \left(g_{11}^i g_{22}^i + g_{12}^i g_{21}^i \frac{g_{32}^i}{g_{31}^i} \right) \left(g_{41}^i g_{52}^i + g_{42}^i g_{51}^i \frac{g_{62}^i}{g_{61}^i} \right)$$
$$+ \tag{13}$$
$$\sin^2\theta \left(g_{11}^i g_{52}^i + g_{42}^i g_{21}^i \frac{g_{62}^i}{g_{31}^i} \right) \left(g_{41}^i g_{22}^i + g_{12}^i g_{51}^i \frac{g_{32}^i}{g_{61}^i} \right)$$
$$= 0$$

The functions that comprise the function G_2^i and its related functions are given in Eqs. (8)–(12) and in the equations below.

$$g_{4k}^i = \sin \eta_k^i L_k \qquad (14)$$

$$g_{5k}^i = \sin \eta_k^i L_{k1} \sin \eta_k^i L_{k2} \qquad (15)$$

$$g_{6k}^i = E_k A_k \eta_k^i \qquad (16)$$

$$\eta_k^i = 2\pi f_i \sqrt{\frac{\rho_k A_k}{E_k A_k}} \qquad (17)$$

The natural frequency f_i is not included explicitly in Eq. (13), but is included in α_k^i, β_k^i, and η_k^i in Eqs. (11), (12), and (17), respectively. In conclusion, Eq. (13) represents a constraint equation that the natural frequency in the in-plane direction must satisfy.

2.5 Previously Proposed Methods [15]

2.5.1 Method 1(out-of-plane method)

The authors previously proposed a tension estimation method (method 1) using the natural frequencies in the out-of-plane direction that is used to solve the following optimization problem:

$$minimize\ F_1(T_1, T_2, E_1 I_1, E_2 I_2) = \sum_{i=1}^{n} \left(G_1^i\right)^2 \qquad (18)$$

where n is the total number of natural frequencies used for the estimation.

The mass per unit length of the two cables $\rho_k A_k$ (density: ρ_k; cross-sectional area: A_k) and the cable length L_k must be determined in advance from the design drawings. The natural frequency f_i is then obtained by measurement. By substituting the measured natural frequency f_i into Eqs. (11) and (12), and then solving the nonlinear optimization problem in Eq. (18), the tension T_k and bending stiffness $E_k I_k$ are obtained for the two cables.

2.5.2 Method 2 (in-plane method)

The authors also previously proposed a tension estimation method (method 2) using the natural frequencies in the in-plane direction that is used to solve the following optimization problem:

$$minimize\ F_2(T_1, T_2, E_1 I_1, E_2 I_2, E_1 A_1, E_2 A_2)$$
$$= \sum_{i=1}^{n} \left(G_2^i\right)^2 \qquad (19)$$

By substituting the measured f_i into Eqs. (11), (12), and (17), and then solving the nonlinear optimization problem in Eq. (19), the tension T_k, bending stiffness $E_k I_k$, and axial stiffness $E_k A_k$ are obtained for the two cables.

2.6 Newly Proposed Methods

2.6.1 Method 3

In methods 1 and 2, only the natural frequencies in the corresponding (i.e., out-of-plane or in-plane) direction can be input into the equations, and the natural frequencies in the other direction cannot be input. This study proposes a new tension estimation method (method 3) that can combine the natural frequencies in both directions. The vibration direction of each natural frequency must be assigned correctly. Method 3 is used to solve the following optimization problem:

$$minimize\ F_3(T_1, T_2, E_1 I_1, E_2 I_2, E_1 A_1, E_2 A_2)$$
$$= \sum_{i=1}^{n1} \left(G_1^i\right)^2 + \sum_{i=1}^{n2} \left(G_2^i\right)^2 \qquad (20)$$

where $n1$ and $n22$ arethe total numbers of natural frequencies for the out-of-plane and in-plane directions, respectively.

2.6.2 Method 4

By installing accelerometers that act in the out-of-plane direction and striking the cable with a hammer in the out-of-plane direction, it becomes theoretically possible to measure the vibrations in the out-of-plane direction. Similarly, by installing accelerometers that act in the in-plane directions and striking the cable with the hammer in the in-plane directions, it becomes theoretically possible to measure the vibrations in the in-plane directions.

However, it is sometimes difficult to excite purely out-of-plane and in-plane vibrations in field measurements. Similarly, it is sometimes difficult to install accelerometers to act in the exact out-of-plane or in-plane directions. In these cases, the vibration direction of the measured natural frequency cannot be specified correctly.

To overcome this difficulty, method 4, which does not need the direction to be specified, is proposed in this work. Method 4 is used to solve the following optimization problem:

$$minimize\ F_4(T_1, T_2, E_1 I_1, E_2 I_2, E_1 A_1, E_2 A_2)$$
$$= \sum_{i=1}^{n} \left(G_1^i \cdot G_2^i\right)^2 \qquad (21)$$

where n is the total number of natural frequencies used for the estimation.

3. NUMERICAL VERIFICATION

3.1 Overview

In this section, numerical simulations are performed to compare the validity of the previously proposed methods (1 and 2) and the newly proposed methods (3 and 4). The natural frequencies obtained by performing an eigenvalue analysis using the finite element method are input into the proposed

methods, and it is then verified whether these methods can estimate the tension. Methods 1, 2, 3, and 4 solve the optimization problems shown in Eqs. (18), (19), (20), and (21), respectively. Because the estimation accuracy for both the bending and axial stiffness is poor [15], only the accuracy of the tension estimation is examined here.
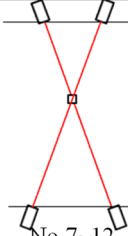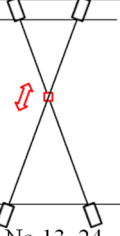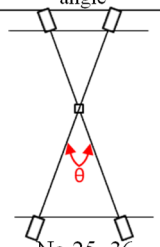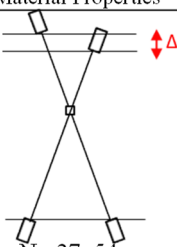
3.2 Analytical Models

Various models for configurations of two cables with an intersection clamp are considered here. About the material properties of the cables, four cable types, which are designated A, B, C, and D, are considered and have properties as shown in Table 1. About the possible combinations of two cables, the five cases listed from Case 1 to Case 5 are considered, as shown in Table 2. In Case 1, the two cables have the same length and the same material properties. In Case 2, the two cables have the same length but different material properties. Cases 3 and 4 are both cases with two cables of the same length and the same material properties. In Case 3, the effect of the clamp location is examined.

Table 1 Cable specifications

Cable name	Tension	Bending stiffness	Axial stiffness	Mass per unit length
	T	EI	EA	ρA
	(kN)	(kN×m²)	(kN)	(ton/m)
A	280.5	12.56	233240	0.0102
B	661.5	68.99	550760	0.0242
C	336.0	17.62	278320	0.0122
D	771.0	92.51	640920	0.0281

Table 2 Cases for cable combinations

Case1: Same Length/Same Material Properties	Case2: Same Length/Different Material Properties	Case3 Changing clamp location
No.1~6	No.7~12	No.13~24

Case4 Changing crossing angle	Case5 Different Length/Same Material Properties
No.25~36	No.37~54

In Case 4, the effect of the crossing angle between the two cables is examined. In Case 5, the two cables have the same material properties but have different lengths.

Table 3 Cable models
(a) Case 1

Model no.	Cable name 1	Cable name 2	L_1 (m)	L_{11}/L_1	θ (°)	L_2/L_1
1	A	A	10	0.6	60	1
2	A	A	20	0.6	60	1
3	A	A	40	0.6	60	1
4	B	B	10	0.6	60	1
5	B	B	20	0.6	60	1
6	B	B	40	0.6	60	1

(b) Case 2

Model no.	Cable name 1	Cable name 2	L_1 (m)	L_{11}/L_1	θ (°)	L_2/L_1
7	A	C	10	0.6	60	1
8	A	C	20	0.6	60	1
9	A	C	40	0.6	60	1
10	B	D	10	0.6	60	1
11	B	D	20	0.6	60	1
12	B	D	40	0.6	60	1

(c) Case 3

Model no.	Cable name 1	Cable name 2	L_1 (m)	L_{11}/L_1	θ (°)	L_2/L_1
13	A	A	10	0.3	60	1
14	A	A	10	0.9	60	1
15	A	A	20	0.3	60	1
16	A	A	20	0.9	60	1
17	A	A	40	0.3	60	1
18	A	A	40	0.9	60	1
19	B	B	10	0.3	60	1
20	B	B	10	0.9	60	1
21	B	B	20	0.3	60	1
22	B	B	20	0.9	60	1
23	B	B	40	0.3	60	1
24	B	B	40	0.9	60	1

(d) Case 4

Model no.	Cable name 1	Cable name 2	L_1 (m)	L_{11}/L_1	θ (°)	L_2/L_1
25	A	A	10	0.6	50	1
26	A	A	10	0.6	70	1
27	A	A	20	0.6	50	1
28	A	A	20	0.6	70	1
29	A	A	40	0.6	50	1
30	A	A	40	0.6	70	1
31	B	B	10	0.6	50	1
32	B	B	10	0.6	70	1
33	B	B	20	0.6	50	1
34	B	B	20	0.6	70	1
35	B	B	40	0.6	50	1
36	B	B	40	0.6	70	1

(e) Case 5

Model no.	Cable name 1	Cable name 2	L_1 (m)	L_{11}/L_1	θ (°)	L_2/L_1
37	A	A	10	0.6	60	0.75
38	A	A	10	0.6	60	0.85
39	A	A	10	0.6	60	0.95
40	A	A	20	0.6	60	0.75
41	A	A	20	0.6	60	0.85
42	A	A	20	0.6	60	0.95
43	A	A	40	0.6	60	0.75
44	A	A	40	0.6	60	0.85
45	A	A	40	0.6	60	0.95
46	B	B	10	0.6	60	0.75
47	B	B	10	0.6	60	0.85
48	B	B	10	0.6	60	0.95
49	B	B	20	0.6	60	0.75
50	B	B	20	0.6	60	0.85
51	B	B	20	0.6	60	0.95
52	B	B	40	0.6	60	0.75
53	B	B	40	0.6	60	0.85
54	B	B	40	0.6	60	0.95

Table 4 Numbers of natural frequencies in each direction and numbers of unknowns

Methods	No. of natural frequencies Out-of-plane	No. of natural frequencies In-plane	No. of unknowns
1	7	0	4 (T_1, T_2, E_1I_1, E_2I_2)
2	0	7	6 ($T_1, T_2,$ $E_1I_1, E_2I_2,$ E_1A_1, E_2A_2)
3	4	3	
4	4	3	

Table 5 Solution ranges (numerical verification)

Parameter	Lower bound	Upper bound
Tension	0.26 × the true value	2 × the true value
Bending stiffness	0.26 × the true value	2 × the true value
Axial stiffness	0.26 × the true value	2 × the true value

A total of 54 analytical models are considered, as shown in Table 3. The two cables were named cable 1 and cable 2. There are three lengths for cable 1 (10 m, 20 m, and 40 m), four combinations of material properties are used for cables 1 and 2 (A-A, B-B, A-C, and B-D), and three different intersection clamp locations (30%, 50%, and 90% from the end), three different cable crossing angles (50°, 60°, and 70°), and four ratios for the two cable lengths (1.0, 0.95, 0.85, and 0.75). Tension estimation was performed for all 54 models.

3.3 Calculation of Natural Frequencies

The natural frequencies of the 54 analytical models were calculated by performing an eigenvalue analysis using the finite element method. Two-dimensional analytical models for the out-of-plane and in-plane directions were then created. The

element size was set at 0.1 m. The boundary condition at both ends was that of simple support. It was assumed that the displacements at the intersection clamp have the same degree of freedom for the two cables.

3.4 Analysis Condition for Tension Estimation

Table 4 shows the number of natural frequencies used to perform the estimation. In all four methods, seven natural frequencies were input in total. Table 4 also shows the number of unknowns for each method.

Table 5 shows the lower and upper bounds for the unknowns when solving the optimization problems. To avoid local minimum solutions, the lower bound for the tension was set to be 0.26 times the true value [15]. In the previous study by Harada et al. [16], the difference between the actual cable tension of a Nielsen-Lohse bridge after 30 years of service and the designed value was approximately 10% on average, and the minimum and maximum ratios of the actual tension to the designed value were 0.76 and 1.4, respectively. Therefore, it is reasonable to set the lower bound for the tension to be 0.26 times the true value and the corresponding upper bound to be twice the true value.

The MultiStart method [17] is used to avoid finding a local minima solution when solving optimization problems. In the MultiStart method, the parameters are estimated using various initial values. The optimal solution is then obtained for each initial value, and the solution with the smallest objective function value is considered to be the optimal global solution. The number of initial values for the MultiStart method was set at 100, and 100 sets of initial values were generated at random within the solution ranges shown in Table 5.
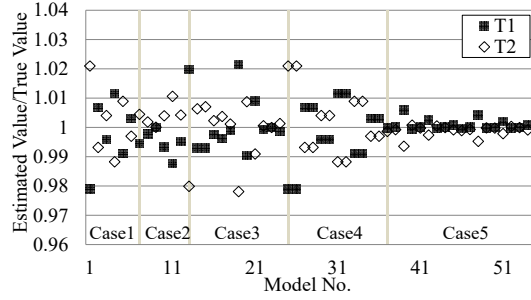
3.5 Tension Estimation Results and Discussion
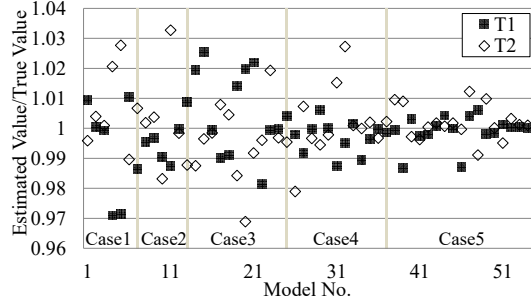
3.5.1 Tension estimation results

Figures 3 (a)-(d) show the tension estimation results for the four methods. The horizontal axis represents the model number, and the vertical axis represents the ratio of the estimated value to the true value. The vertical grid lines represent the boundaries between the cases. When the estimated value on the vertical axis is closer to 1, this indicates that the estimate is closer to the true value.

Figure 3(e) compares the average, maximum and minimum values of the estimation results (the ratio of the estimated value to the true value) for the four methods. The average is expressed with bars and almost 1 for all methods. The maximum and minimum values are expressed with error bars. The maximum estimation errors for methods 1, 2, 3, and 4 are 2.2%, 3.3%, 2.3%, and 2.6%, respectively. Method 1 shows the highest accuracy, and Method
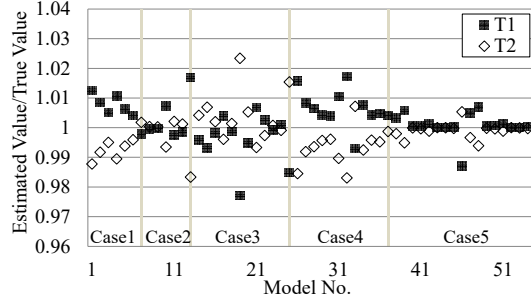
2 shows the lowest accuracy. However, all methods show comparatively high accuracy for all models.
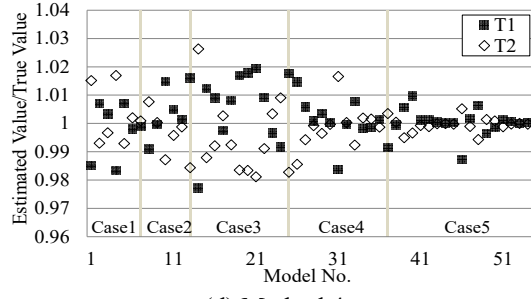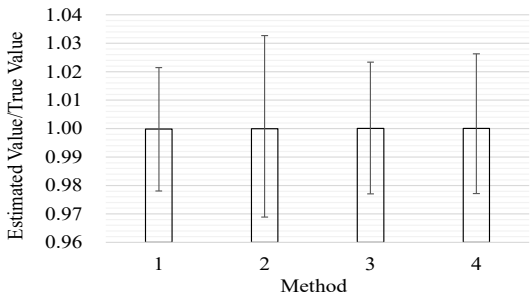

(a) Method 1

(b) Method 2

(c) Method 3

(d) Method 4

(e) Comparison of average, maximum, and minimum values

Fig. 3 Tension estimation results for methods 1–4

3.5.2 Tension estimation errors

Figures 4 (a)-(d) show the tension estimation errors for the four methods.

For method 1, the tension estimation errors of the two cables are almost the same as shown in Fig. 4(a). From Fig. 3(a) and 4(a), it was found that the tension of one cable is underestimated, while the tension of the other cable is overestimated by the same amount. This is because the natural frequencies of the two cables do not change significantly if the tension of one cable is slightly reduced and the tension of the other cable is increased by the same amount. Furthermore, the estimation errors of model no. 1-36 is larger than those of model no. 37-54. The shape of model no. 1-36 is symmetrical with two cables having the same cable length, whereas the shape of model no. 37-54 is asymmetrical with different cable lengths. The situation where the tension of one cable is underestimated and the tension of the other cable is overestimated is likely to occur in the symmetric models. In addition, the models with short cables (10m) tend to have a large estimation error.

For method 2, on the other hand, the tension estimation errors of the two cables are different, as shown in Fig. 4(b). Method 2 uses in-plane natural frequencies that are affected by the axial stiffness in addition to tension and bending stiffness, whereas method 1 uses out-of-plane natural frequencies that are only affected by tension and bending stiffness. Therefore, tension is less sensitive to the in-plane natural frequencies used in method 2 than the out-of-plane natural frequencies used in method 1. Therefore, the tension estimation error of method 2 is larger than that of method 1, and the estimation error of the two cables is different in method 2.

Methods 3 and 4 use the simultaneous input of both out-of-plane and in-plane natural frequencies. Figures 3(c) and 3(d) show that the estimation errors of the two cables are almost the same, showing a similar tendency to method 1. Figure 4(e) compares the tension estimation errors among the four methods using three error indices. The maximum error is the maximum estimation error for all models and both cables. The root-mean-square error ratio (RMSER) and the maximum absolute error ratio (MAER) were calculated as follows:

$$RMSER = \sqrt{\frac{1}{2N}\sum_{I=1}^{N}\sum_{k=1}^{2}\left(\frac{T_k^{estimated}(I)}{T_k^{true}(I)}-1\right)^2} \quad (22)$$

$$MAER = \frac{1}{2N}\sum_{I=1}^{N}\sum_{k=1}^{2}\left|\frac{T_k^{estimated}(I)}{T_k^{true}(I)}-1\right| \quad (23)$$

where N is the total number of cables (54), T_1^{true} and T_2^{true} are the true values of the tension of cables 1 and 2, respectively, $T_1^{estimated}$ and $T_2^{estimated}$ are the estimated tensions of cables 1 and 2, respectively, and I is the model number.

(a) Method 1

(b) Method 2

(c) Method 3

(d) Method 4
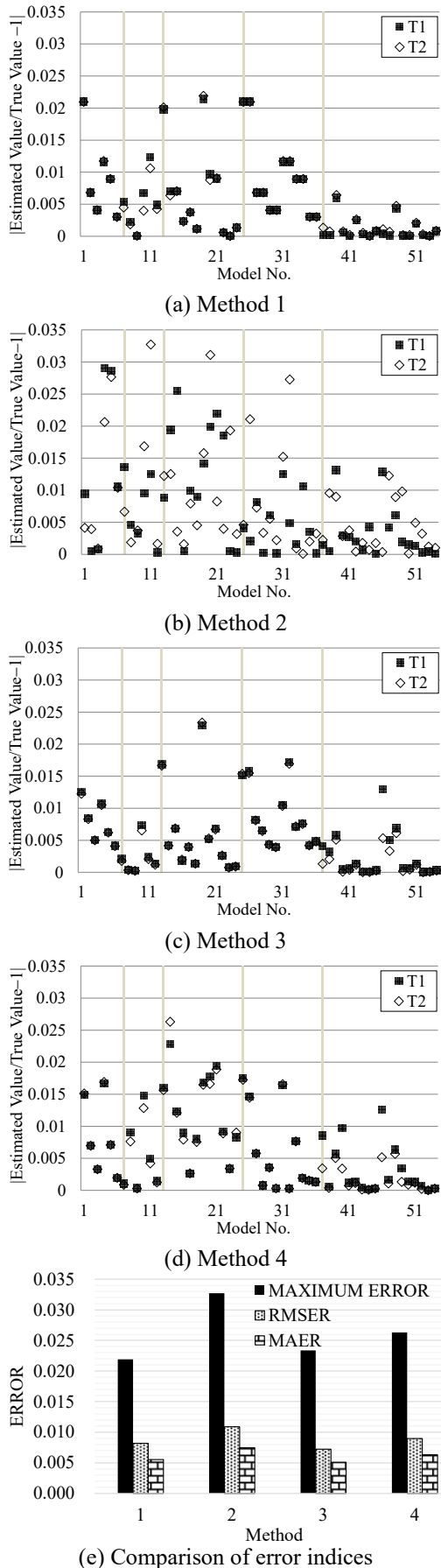

(e) Comparison of error indices

Fig. 4 Tension estimation errors for methods 1–4

If the methods are listed in ascending order of maximum error, the order is method 1 < method 3 < method 4 < method 2. If the methods are listed in ascending order of RMSER and MAER, the order becomes method 3 < method 1 < method 4 < method 2. Method 1 gives the smallest maximum error, and method 3 gives the smallest average error. Method 4 is the third most accurate method, and method 2 shows the lowest accuracy. Methods 3 and 4 both showed higher accuracy than method 2 because they use the natural frequencies in out-of-plane directions. Method 4 showed high accuracy even though it does not specify the vibration directions for the natural frequencies.

Based on the findings above, the use of method 1 is recommended if the vibration directions of the measured natural frequencies can be specified correctly, and the use of method 4 is recommended if the vibration directions of the measured natural frequencies are difficult to specify.

4. EXPERIMENTAL VERIFICATION

4.1 Outline of Experiment

Physical model experiments were conducted to validate the proposed methods. A schematic diagram of the setup used and photographs of the test specimen are shown in Fig. 5. Two cables were connected by an intersection clamp and supported at both ends. Prestressed steel strands were used for the cables. A load cell was installed at one end of each cable, and the tensions measured using these load cells were assumed to be the true values. Accelerometers were installed in each span between the intersection clamp and each cable end.

Table 6 lists the structural specifications of the test specimen. The tensions shown in Table 6 are the values measured using the load cells. The bending stiffness and axial stiffness were determined through the multiplication of the catalog values of Young's modulus and the cross-sectional properties.

4.2 Natural Frequency

In the experiments, the test specimen was struck with a hammer near accelerometer no. 1. The natural frequencies were then obtained by reading the dominant frequencies from the acceleration Fourier spectra. The natural frequencies in the out-of-plane and in-plane directions are listed in Table 7 in ascending order. The natural frequencies in the out-of-plane and in-plane directions were obtained from accelerometers installed in the corresponding directions. The number of natural frequencies used in the estimation process is shown in Table 4. It is the same number that was used in the numerical verification. In each of the methods, seven natural frequencies were input in total.
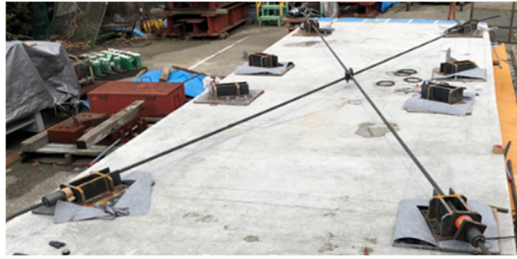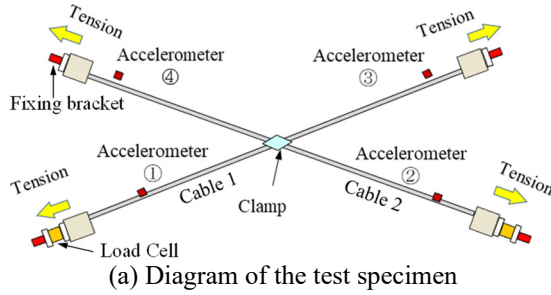
(a) Diagram of the test specimen

(b) Photograph of the test specimen

(c) Cable cross-section (d) Intersection clamp
Fig. 5. Overview of the model experiment

Table 6 Parameters of the test specimen

Cable no.	Tension (kN)	Bending stiffness (kN·m²)	Axial stiffness (kN)	Mass per unit length (ton/m)
1	T_1	$E_1 I_1$	$E_1 A_1$	$\rho_1 A_1$
	150.4	2.26	1.04×10^5	0.0043
2	T_2	$E_2 I_2$	$E_2 A_2$	$\rho_2 A_2$
	103.6	2.26	1.04×10^5	0.0043

Cable no.	Length (m)	Location of the intersection clamp (-)	Cable crossing angle θ (°)
1	L_1	L_{11}/L_1	
	7.836	0.5	40
2	L_2	L_{22}/L_2	
	7.835	0.5	

Table 7 Observed natural frequencies

Out-of-plane (Hz)	11.33	24.41	25.90	35.08	51.76	78.16	82.58
In-plane (Hz)	11.25	25.59	34.77	52.46	61.21	81.80	111.48

Table 8 Solution ranges (experimental verification)

Parameter	Lower bound	Upper bound
Tension	0.26 × the true value	2 × the true value
Bending stiffness	1	10 × the designed value
Axial stiffness	1	10 × the designed value

Table 9 Tension estimation results

Method	T_1 (kN) (estimated /true)	T_2 (kN) (estimated /true)	Maximum error	Averaged error
1	165.4 (1.100)	103.7 (1.001)	0.1	0.05
2	169.0 (1.124)	73.2 (0.707)	0.29	0.21
3	142.7 (0.949)	29.7 (0.287)	0.71	0.38
4	152.8 (1.016)	111.1 (1.073)	0.07	0.04

4.3 Solution Ranges

The solution ranges used to solve the optimization problem were set as shown in Table 8. Because the designed values of the bending and axial stiffnesses are not the exact values, the ranges for the bending and axial stiffness were extended. As a result of this extension of the ranges of the bending and axial stiffnesses, the number of initial values for the MultiStart method was set at 1000.

4.4 Tension Estimation Results and Discussion

Table 9 presents the tension estimation results. If the methods are listed in ascending order of the maximum and averaged errors, the order is method 4 < method 1 < method 2 < method 3.

Although the accuracy of method 1 is inferior to that of method 4, the difference between their maximum errors is not significant, and the estimation accuracy of method 1 for cable 2 is quite high. Therefore, the vibration direction for the observed natural frequencies for the out-of-plane direction is considered to have been assigned correctly.

Because method 2 showed lower accuracy when compared with methods 1 and 4, it is considered that some of the observed natural frequencies assigned to the in-plane direction may be natural frequencies in the out-of-plane direction. Since method 3, which used the three lowest in-plane natural frequencies, showed the lowest accuracy, it is thus possible that a natural frequency with a direction that was erroneously assigned may have been included among the three lowest natural frequencies assigned to the in-plane direction.

The out-of-plane deformation is resisted by the tension and bending stiffness of the cables. In contrast, the in-plane deformation is resisted by the axial stiffness of the cables, in addition to the tension and bending stiffness. Therefore, the out-of-plane natural frequencies are more reliable because the out-of-plane vibrations are easier to generate, and the in-plane natural frequencies are less reliable because in-plane vibrations are less likely to be generated. This may be the reason why method 1 (which uses natural frequencies in the out-of-plane direction only) and method 4 (which does not specify the vibration direction for natural

frequencies) showed high accuracy. From the findings above, the use of methods 1 and 4 is recommended.

5. CONCLUSIONS

In Nielsen-Lohse bridges, braced cables cross each other and are connected by intersection clamps. In the current practice for cable tension estimation, these intersection clamps are removed, a vibration-based cable tension estimation method for use on single cables is applied to each cable, and the intersection clamps are then reinstalled. To improve the efficiency of this inspection work, the authors previously proposed two tension estimation methods (methods 1 and 2) that could be used without removing the intersection clamps. Method 1 estimates the tension based on the natural frequencies acting in the out-of-plane direction. Method 2 estimates the tension based on the natural frequencies acting in the in-plane direction. However, collection of the required number of natural frequencies in each direction and specification of the vibration direction for each natural frequency can occasionally be difficult.

This study, therefore, proposes additional methods 3 and 4, which allow simultaneous input of both the out-of-plane and in-plane natural frequencies. The difference between these methods is that method 3 requires the vibration direction for each natural frequency but method 4 does not.

The validity of both methods was verified using numerical simulations and experiments. The findings of this study are discussed below.

In the numerical simulations, the validity of each of the proposed methods was verified using 54 models with different material properties, cable lengths, intersection clamp locations, crossing angles, and cable length ratios. Method 1 showed the highest accuracy and method 2 showed the lowest accuracy among the four methods. Method 4 showed higher accuracy than method 2 even though it does not require the vibration direction to be specified. Therefore, the use of method 1 is recommended if the vibration direction can be specified correctly, and the use of method 4 is recommended if the vibration direction is difficult to specify.

Experiments were also performed to verify the proposed methods. The results showed that methods 1 and 4 showed high accuracy, but methods 2 and 3 showed low accuracy. From the comparison, it was speculated that the natural frequencies in the out-of-plane direction were more reliable because out-of-plane vibrations are more likely to occur, and the natural frequencies in the in-plane direction are less reliable because in-plane vibrations are less likely to occur. It was found that there is a possibility that natural frequencies in the in-plane direction are erroneously assigned as those in the out-of-plane direction. Therefore, it can be inferred that method 1, which used only out-of-plane natural frequencies, and method 4, in which the vibration direction is not specified, showed the highest accuracy.

Following both the numerical and experimental verifications, it was concluded that methods 1 and 4 are recommended. However, the test cases are limited. In future work, we hope to perform verification tests on actual bridges.

6. REFERENCES

[1] Shinke, T., Hironaka, K., Zui, H., Nishimura, H. (1980). Practical formulas for estimation of cable tension by vibration method. Journal of Japan Society of Civil Engineers 294, 25-32. (In Japanese)

[2] Yamagiwa, I., Utsuno, H., Endo, K., Sugii, K. (2000). Identification of flexural rigidity and tension of one-dimensional structure by measuring eigenvalues in higher order. Transactions of the Japan Society of Mechanical Engineers 66:649, 2905-2911. (In Japanese)

[3] Chen, C.C., Wu, W.H., Leu, M.R., Lai, G. (2016). Tension determination of stay cable or external tendon with complicated constraints using multiple vibration measurements. Measurement 86, 182-195.

[4] Chen, C.C., Wu, W.H., Leu, M.R., Lai, G. (2018). A novel tension estimation approach for elastic cables by elimination of complex boundary condition effects employing mode shape functions. Engineering Structures 166, 152-166.

[5] Yan, B., Chen., W., Yu, J., Jiang, X. (2019). Mode shape-aided tension force estimation of cable with arbitrary boundary conditions. Journal of Sound and Vibration 440, 315-331.

[6] Ma, L. (2017). A highly precise frequency-based method for estimating the tension of an inclined cable with unknown boundary conditions. Journal of Sound and Vibration 409, 65-80.

[7] Zarbaf, S.E.H.A.M., Norouzi, M., Allemang, R., Hunt, V., Helmicki, A., Venkatesh, C. (2018). Vibration-based cable condition assessment: A novel application of neural networks. Engineering Structures 177, 291-305.

[8] Furukawa, A., Hirose, K., Kobayashi, R. (2021). Tension estimation method for cable with damper using natural frequencies, Frontiers in the built environment, Vol.7, Article 603857.

[9] Furukawa, A., Hirose, K., Kobayashi, R. (2021). Tension estimation method for cable with damper and its application to the real cable-stayed bridge, Proceedings of the 9th international conference on experimental vibration analysis for civil engineering

structures, Paper No. S8-1.

[10] Furukawa, A., Suzuki, S., Kobayashi, R. (2022). Tension estimation method for cable with damper using natural frequencies with uncertain modal order, Frontiers in the built environment, Vol,8, Article 812999.

[11] Kitada, T., Nakai, H., Yoshikawa, O., Sakano, M. (1988). A rational design method for buckling the arch-ribs of the Nielsen-Lohse bridge. Journal of Structural Engineering, JSCE 34A, 315-326.

[12] Yoneda, M. (2000). Effect of lifting materials on the structural damping of Nielsen-type Lohse-girder bridges. Proceedings of the Civil Engineering Society 651:IV-47, 157-162.

[13] Sakano, M., Kitada, T., Chono, K. (2003). Mechanical properties of Nielsen-Lohse bridges and their load-bearing capacity. Proceedings of the Society of Civil Engineers on Structural Engineering 49A, 93-104.

[14] Kuriyama, T. Bing, Y., Horiuchi, H. (1994). A proposal for a tension measurement method for cable with clamps on Nielsen bridge. The 49th Annual lecture of the civil engineering society (CSC) I-176, 350-351.

[15] Furukawa, A., Yamada, S., Kobayashi, R. (2022). Tension estimation methods for two cables connected by an intersection clamp using natural frequencies. Journal of Civil Structural Health Monitoring 12, 339-360.

[16] Masahiko, H. Yasuo, K., Saiji, F. (2002). Survey of the Nielsen-Lohse bridge after 30 years. Civil Engineering Society 57th Annual Academic Lecture I-290, 579-80. (In Japanese)

[17] MathWorks. (2022). Matlab Documentation, MultiStart, https://jp.mathworks.com/help/gads /multistart.html [Accessed: January 10, 2022].